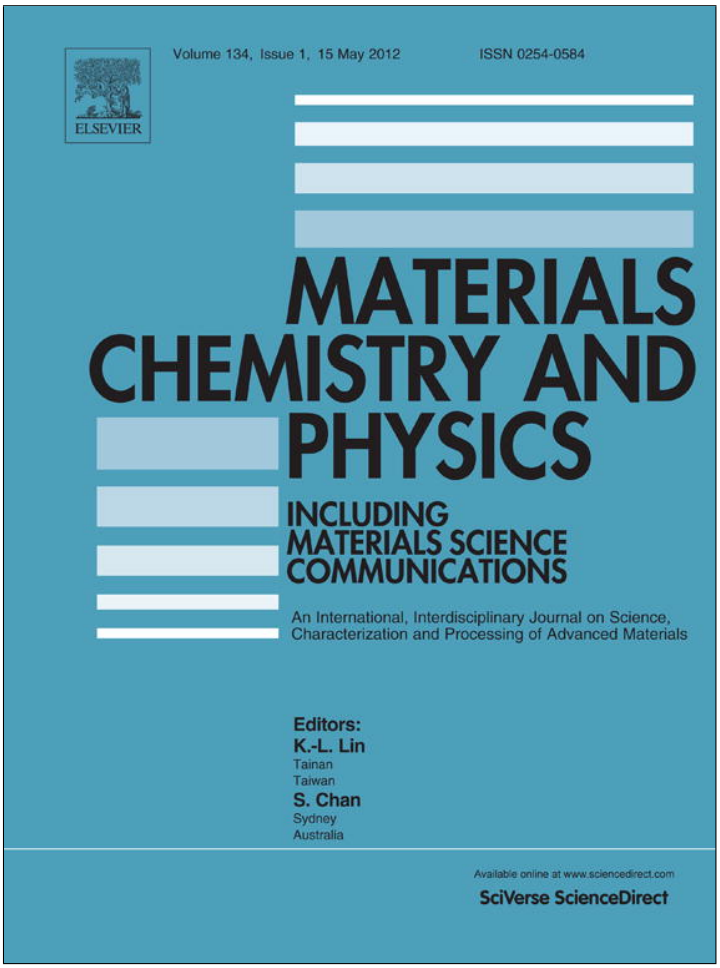

Materials Chemistry and Physics 134 (2012) 371–376

Contents lists available at SciVerse ScienceDirect

Materials Chemistry and Physics

journal homepage: www.elsevier.com/locate/matchemphys

Effect of magnesium chloride on growth, crystalline perfection, structural, optical, thermal and NLO behavior of γ-glycine crystals

G.R. Dillip[a], G. Bhagavannarayana[b], P. Raghavaiah[c], B. Deva Prasad Raju[d,*]

[a] Department of Physics, Sri Venkateswara University, Tirupati 517 502, India
[b] Materials Characterization Division, CSIR-National Physical Laboratory, New Delhi 110 012, India
[c] School of Chemistry, University of Hyderabad, Hyderabad 500 046, India
[d] Department of Future Studies, Sri Venkateswara University, Tirupati 517 502, India

ARTICLE INFO

Article history:
Received 5 February 2011
Received in revised form 8 December 2011
Accepted 1 March 2012

PACS:
81.10.Dn
42.70.Mp
65.40.−b
78.20.Ci

Keywords:
Crystal growth
FTIR
Optical properties
Thermal properties

ABSTRACT

In the present study, single crystals of γ-glycine possessing excellent non-linear optical properties were successfully grown at room temperature in the presence of magnesium chloride ($MgCl_2$) for the first time by using the slow solvent evaporation method. The second harmonic conversion efficiency of γ-glycine crystal was determined using Kurtz powder technique with Nd:YAG laser and was found to be 6 times greater than that of the standard inorganic sample potassium dihydrogen phosphate (KDP). The crystalline perfection of the grown crystal was analyzed using high-resolution X-ray diffraction (HRXRD) rocking curve measurements. The grown crystal was subjected to single crystal XRD and powder XRD, which confirmed that the crystal has hexagonal structure and belongs to space group $P3_1$. Inductively coupled plasma optical emission spectrometry (ICP-OES) was carried out to quantify the concentration of Mg element in the grown γ-glycine single crystal. Fourier transform infrared (FTIR) spectral studies were made to identify the functional groups. The optical band gap was likewise estimated for γ-glycine crystal using UV–vis–NIR study. The optical measurements of γ-glycine crystal helped to calculate the optical constants such as refractive index (n), the extinction coefficient (K), electric susceptibility (χ_c) and both the real ($\in_r$) and imaginary ($\in_i$) components of the dielectric permittivity functions of photon energy, which is essentially required to develop optoelectronic devices. Thermogravimetric analysis (TGA) and differential thermal analysis (DTA) were used to study thermal stability and decomposition point of the grown crystal.

1. Introduction

The potential applications of non-linear optical materials in the emerging fields of photonic, fiber optic communications, frequency doubling and optical signal processing areas has attracted the attention of scientists [1,2]. The efficient optical frequency conversion of NLO crystals is the key step in the development of laser systems. These systems are of great importance as wide range tunable sources of coherent illumination in UV, vis and NIR spectral regions. Recent investigations focus on the design of a novel material that can reach second order optical processes, and have strong interaction with the oscillating electric field of light [3]. Till now in the fields of non-linear optical materials much attention has been devoted towards the preparation and optimization of novel optical materials and also they have become more significant because of their function in various photonic devices. In order to identify new optical devices for specific utility, or devices with enhanced performance, active research is being carried out by choosing appropriate non-linear optical materials [4,5].

Organic materials are optically more non-linear than inorganic materials because these are formed by weak Van der walls and hydrogen bonds that result in poor mechanical strength and possess a high degree of delocalization. The amino acids are the best-known organic materials that play a vital role in the field of non-linear optical crystal growth. The natural amino acids exhibit individual non-linear optical properties as they have a donor NH_2 and acceptor COOH. The γ-glycine shows NLO activity because of the presence of an additional COOH group in the first and another NH_2 group in the second.

A survey of literature shows that the six distinct polymorphic forms of glycine can be formed under different solution conditions: α-, β- and γ-forms in ambient environment and δ-, ∈- and β^1-forms under high pressure conditions [6–8]. Both α and β-glycine polymorphs crystallize in centrosymmetric space group $P2_1/m$ and hence they do not exhibit second harmonic generation, while γ-form of glycine crystallizes in the trigonal–hexagonal system with

* Corresponding author. Tel.: +91 94402 81769.
E-mail address: drdevaprasadraju@gmail.com (B. Deva Prasad Raju).

0254-0584/$ – see front matter © 2012 Elsevier B.V. All rights reserved.
doi:10.1016/j.matchemphys.2012.03.004

non-centrosymmetric space group of $P3_1$ structure making it a suitable candidate for piezoelectric, electro optic and non-linear optical applications [9–11]. α-Glycine can be formed from spontaneous nucleation of pure aqueous glycine. The least stable β-form of glycine can be formed using mixed solvents such as methanol or ethanol and water. γ-Glycine is the thermodynamically most stable form at room temperature. It is produced from acidic (pH 3.40) and basic (pH 10.10) solutions. Moreover, it can be crystallized with additives in neutral aqueous solutions. At 1.9 GPa γ-glycine begins to undergo a transition to form high-pressure phase ∈-glycine. The transition from ∈-glycine to a new phase of glycine (δ-glycine) begins to occur at 2.74 GPa and the β^1-form at 0.76 GPa. In solid state, γ-glycine exists as a dipolar ion in which carboxylic group is present as carboxylate ion and amino group are present as ammonium ion. Due to this dipolar nature, glycine has a high melting point. In addition to this, the presence of chromophores namely amino group and carboxyl group make the γ-glycine crystal transparent in the UV–vis region. Thus, the investigation in the suitable environment in which glycine crystallizes into γ-form gains importance. The growth of γ-glycine crystals with (i) sodium chloride (ii) sodium hydroxide (iii) sodium fluoride (iv) phosphoric acid (v) lithium acetate and (vi) lithium bromide from the aqueous solutions of glycine has been reported and the effect of these additives on its various physical characteristics analyzed [12–15]. In this paper, we report the effect of magnesium chloride on the growth of γ-glycine for the first time, as some of the physical properties of the reported γ-glycine crystals get enhanced by this solvent. The characterization studies such as HRXRD, single crystal XRD, powder XRD, Fourier transform infrared (FTIR) analysis, UV–vis–NIR spectroscopic analysis, TGA/DTA, ICP-OES analysis and NLO studies have been carried out.

2. Material synthesis

Single crystals were obtained at room temperature from saturated solutions containing molar ratios that are the same as those of their components by using the slow evaporation method. The analytical grade (AR) α-glycine and magnesium chloride supplied by MERCK, India were taken in 2:1 stoichiometric ratio as the starting materials for synthesis of the title compound. Firstly, the calculated amounts of these materials were dissolved at room temperature in double distilled water and then to attain homogenous mixture the solution stirred well by using magnetic stirrer. It was afterwards filtered twice with Whatmann filter paper to remove impurities. This supersaturated solution was tightly covered with plastic paper to keep out dust before it was slowly allowed to evaporate at room temperature. After a period of 25 days, colorless, transparent crystals up to several millimeters in size were harvested from the mother solution. The grown crystals are shown in Fig. 1.

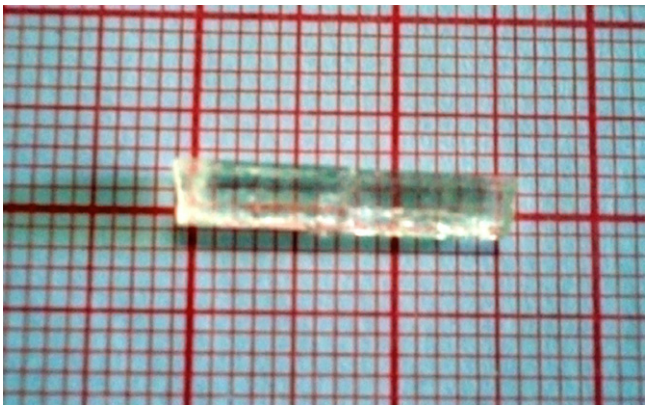

Fig. 1. The grown γ-glycine crystal from magnesium chloride.

3. Results and discussion

3.1. HRXRD studies

High resolution X-ray diffraction studies employing a multicrystal X-ray diffractometer developed at NPL [16] were carried out to examine the crystalline perfection of the grown single crystals. The well-collimated and monochromated $MoK\alpha_1$ beam obtained from the three monochromatic Si crystals set in dispersive (+,−,−) configuration was used as the exploring X-ray beam. The specimen crystal was aligned in the (+,−,−,+) configuration. Due to dispersive configuration, though the lattice constant of the monochromator crystal(s) and the specimen are different, the unwanted dispersion broadening in the diffraction curve (DC) of the specimen crystal is insignificant. The specimen can be rotated with minimum angular interval of 0.4 arc S about the vertical axis, which is perpendicular to the plane of diffraction. The rocking curve was recorded by the so-called ω scan wherein the detector was kept at the same angular position ($2\theta_B$) with a wide opening for its slit [17].

Fig. 2 shows the high-resolution X-ray diffraction curve recorded for a typical γ-glycine single crystal specimen using (1 1 0) diffraction planes with $MoK\alpha_1$ radiation. On careful observation, the curve does not seem to be a single peak. The solid line (convoluted curve) is fitted well with the experimental points represented by the filled circles. On deconvolution of the diffraction curve, it is clear that the curve contains two additional peaks, 60 and 24 arc S that are away from the central peak (the highest intensity peak). These two additional peaks correspond to two internal, structural by very low-angle boundaries whose tilt angles (the misorientation angle between the two crystalline regions on both sides of the structural grain boundary) from their adjoining regions are 60 and 24 arc S. The FWHM (full width at half maximum) of the main peak and the very low angle boundaries are 72, 74 and 550 arc S, respectively. The broadest and low intensity peak shows that the small grain corresponding to this peak contain sub-micron size mosaic blocks misoriented to each other by a few arc minutes. These types of structural defects are probably generated in the crystal due to mechanical/thermal fluctuations occurred during the growth process and/or also due to fast growth [18]. The affect of such very low angle boundaries may not be very significant in many applications, but for applications like phase matching, it is essential to know these minute details with quantitative data of misorientation

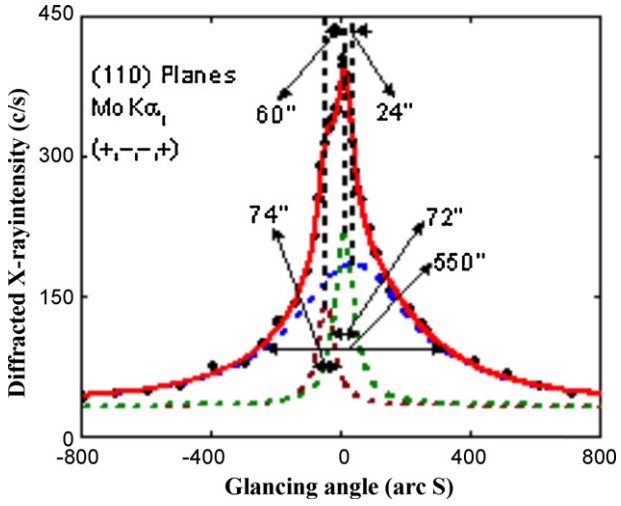

Fig. 2. Rocking curve recorded for γ-glycine single crystal for (1 1 0) diffracting planes by employing the multicrystal diffractometer with $MoK\alpha_1$ radiation.

Table 1
Comparison of lattice parameters of γ-glycine single crystals grown with various additives.

Sample	Lattice parameters		References
	$a = b$ (Å)	c (Å)	
γ-Glycine with H_3PO_4	7.028	5.447	[14]
γ-Glycine with LiBr	7.026	5.475	[15]
γ-Glycine with $MgCl_2$	7.037	5.489	Present work

of the structural grains as a part of the assessment of crystalline perfection. It may be mentioned here that the detection of such very low angle grain boundaries with well-resolved peaks in the diffraction curve in the present study was possible only because of the use of the high-resolution multicrystal X-ray.

3.2. Single crystal XRD and ICP-OES studies

In order to identify the crystal structure and to determine the unit cell parameter values, the grown crystal was subjected to single crystal X-ray diffraction study using Oxford Diffraction Xcalibur Eos Gemini diffractometer with graphite-monochromated Mo $K\alpha$ radiation of the wavelength of 0.71073 Å. Data were analyzed with "CrysAlis PRO" software and the collected data was reduced by using the "CrysAlis PRO" program. An empirical absorption correction using spherical harmonics was implemented in "SCALE3 ABSPACK" scaling algorithm. The crystal structure was solved by direct methods that use SHELXS-97 and the refinement was carried out against F^2 using SHELXL-97 [19,20]. The cell parameter values of γ-glycine crystal were found to be $a = b = 7.037$ Å, $c = 5.489$ Å, $\alpha = \beta = 90^\circ$ and $\gamma = 120^\circ$ and the volume of the unit cell is 235.46 Å^3. Table 1 represents the comparison of lattice parameters of γ-glycine single crystals with various additives and these are in good agreement with the reported values. This indicates that the γ-glycine crystallizes in hexagonal system with $P3_1$ space group, which is recognized as non-centrosymmetric. Thus, it is satisfies one of the basic and essential material requirements for the SHG activity of the crystal [21]. Further, it is evident from this study that the inorganic compound is not incorporated into the lattice cites of the organic host. To determine the concentration of Mg element present in the grown crystal, the authors are carried out the inductively coupled plasma optical emission spectrometry (ICP-OES) analysis of γ-glycine using Perkin Elmer Optima 5300 DV ICP-OES spectrometry. For this analysis, the grown crystal was crushed in pieces and finely grounded in an agate mortar. This powdered sample weighing about 73.86 mg was transferred into a 25 ml volumetric flask with the help of funnel and was brought up to volume with deionized water. This diluted sample was analyzed by ICP-OES. The ICP-OES analysis gave a characteristic wavelength at 285.213 nm which is the fingerprint for magnesium element. Further, these results indicates that the low concentration of magnesium (0.898 mg L^{-1}) present in the grown crystal [22].

3.3. Powder X-ray diffraction analysis

Finely crushed powder of γ-glycine crystal was subjected to powder X-ray diffraction analysis employing a SIEFERT 3003 TT diffractometer with a characteristic CuKα ($\lambda = 1.540598$ Å) radiation for structural analysis. The sample was scanned in the 2θ values from 10° to 60° at a rate of 2° min^{-1}. Fig. 3 shows the XRD profile of the grown crystal. The positions of the peaks were found to be in agreement with the literature available in JCPDS file no: 06-230. The characteristic peak has appeared at around 25.36° (2θ). This study confirms that the existence of glycine in γ-phase.

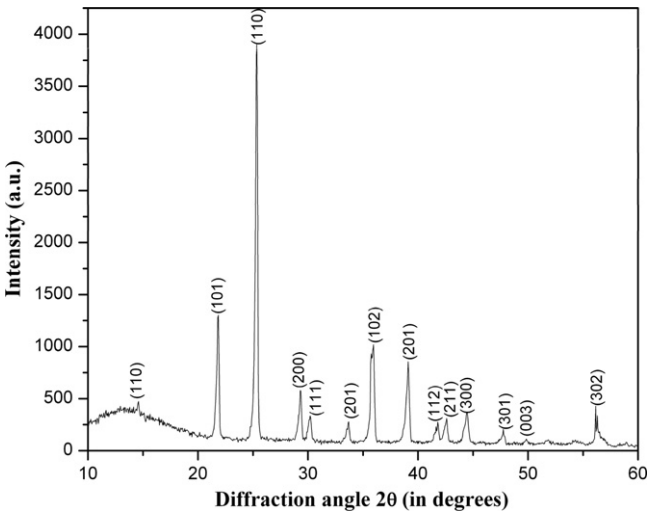

Fig. 3. Powder XRD pattern of γ-glycine crystal.

3.4. FTIR analysis

Fourier transform infrared (FTIR) spectrum was recorded using Perkin-Elmer spectrophotometer in the range 450–4000 cm^{-1} to quantitatively analyze the presence of functional groups in γ-glycine. For this analysis, the sample was taken in pellet form in the KBr phase. The characteristic transmission peaks of infrared spectrum are shown in Fig. 4.

The peaks observed at 686, 607 and 503 cm^{-1} indicated the presence of carboxylate group. The NH_3^+ group is revealed by the peaks observed at 2619, 1497 and 1126 cm^{-1}. These observations confirmed that the glycine molecule exists as zwitterionic form inside the crystal, in which the carboxyl group is present as a carboxylate ion and the amino group is present as an ammonium ion. Thus, the present study evidences the existence of glycine in γ-phase. The peaks at 889, 1391 and 2919 cm^{-1} are attributed to CCN, COO^- and CH_2 stretching groups, respectively. The assignment of vibrations of γ-glycine crystal is shown in Table 2 and these are in good agreement with those in literature [23].

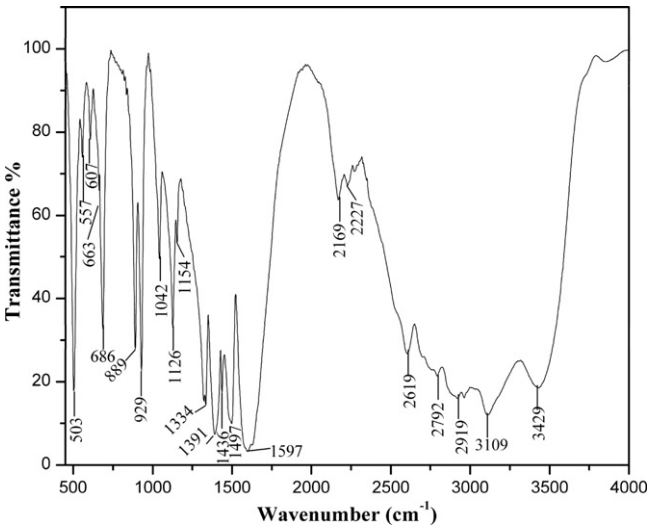

Fig. 4. FTIR spectrum of γ-glycine crystal.

Table 2
Comparion of fundamental vibrations of γ-glycine with α-glycine.

Frequency in wavenumber (cm^{-1})		
α-Glycine	γ-Glycine	Assignment of vibrations
504	503	$-COO^-$ rock
607	607	$-COO^-$ wag
694	686	$-COO^-$ bend
893	889	CCN symmetric stretch
910	929	CH_2 rock
1033	1042	CCN asymmetric stretch
1133	1126	NH_3^+ rock
1333	1334	CH_2 twist
1413	1391	COO^- symmetric stretch
1445	1436	CH_2 bend
1507	1497	NH_3^+
1605	1597	Strong asymmetric CO_2 stretching
2122	2169	Combinational bond
2614	2619	NH_3^+ stretching
3175	3109	NH_3^+ stretching

3.5. Optical absorption study and optical constants calculation

The UV–vis–NIR absorption spectrum of the grown crystal was recorded in the wavelength range 200–1200 nm using Perkin Elmer Lambda 935 UV–vis–NIR spectrometer. The spectrum is shown in Fig. 5. The low absorption in the entire UV and visible region is a potential requirement for NLO applications. The characteristic absorption band that is observed at 238 nm may be attributed to the electronic transitions in the γ-glycine molecule and there is no absorption band between 238 and 1200 nm. The good transmission property of the crystal in the entire visible region suggests its suitability for second harmonic generation. The band gap of the grown crystal was calculated with the help of the optical absorption coefficient of the photon energy [24].

The optical absorption coefficient (α) was calculated from the absorbance (A) using the following relation

$$\alpha = \frac{2.3026 \times A}{t}$$

where t is the thickness of the sample

The relation between the optical band gap (E_g), absorption coefficient and energy ($h\nu$) of the incident photon is given by

$$\alpha h\nu = B(h\nu - E_g)^r$$

where E_g is optical energy gap of the crystal, B is a constant, h is the Planck's constant, ν is the frequency of incident photons and r is an index which can be assumed to have values of 1/2, 3/2, 2 and 3

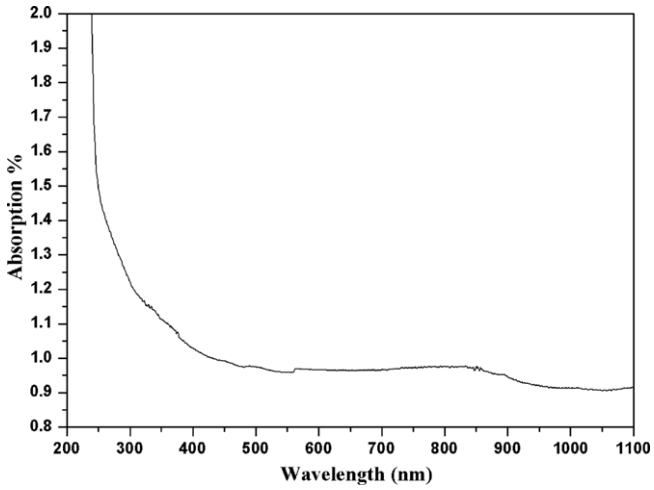

Fig. 5. UV–vis–NIR spectrum of γ-glycine crystal.

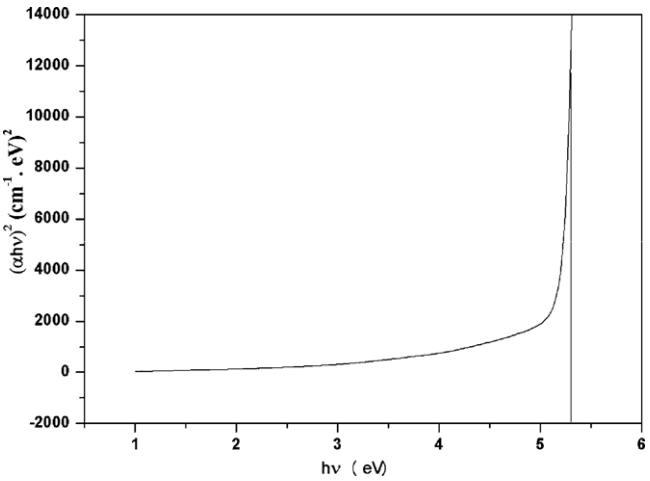

Fig. 6. Plot of $(\alpha h\upsilon)^2$ versus photon energy ($h\upsilon$) of γ-glycine crystal.

depending on the nature of the electronic transition responsible for the absorption. $r = 1/2$ for allowed direct transition, $r = 3/2$ for forbidden direct transition and $r = 3$ for forbidden indirect transition, while $r = 2$ refer to indirect allowed transitions [25].

Owing to the direct band gap, the crystal under study has an absorption coefficient (α) obeying the following relation for high photon energies ($h\nu$)

$$\alpha = \frac{(h\nu - E_g)^{1/2}}{h\nu}$$

The plot of variation of $(\alpha h\nu)^2$ versus $h\nu$ was used to estimate the band gap of the γ-glycine crystal as shown in Fig. 6 and extrapolating the edge to the energy axis from Fig. 6, the value of band gap is obtained as 5.30 eV.

The absorption coefficient (α) is related to the extinction coefficient (K) by

$$\alpha = \frac{4\pi K}{\lambda}$$

The extinction coefficient (K) can be calculated from the above relation,

$$K = \frac{\alpha\lambda}{4\pi}$$

where λ is the wavelength.

The absorption coefficient (α) and the extinction coefficient (K) were obtained from the transmittance (T) and reflectance (R) using approximate formula [26],

$$T = \frac{(1-R)^2 \exp(-\alpha t)}{1 - R^2 \exp(-2\alpha t)}$$

where t is the thickness of the sample.

The refractive index (n) can be determined from the reflectance (R) data using [27],

$$R = \frac{(n-1)^2}{(n+1)^2}$$

The reflectance in terms of absorption coefficient can be obtained from the above relation [28]. Hence,

$$R = 1 \pm \frac{\sqrt{1 - \exp(-\alpha t) + \exp(\alpha t)}}{1 + \exp(-\alpha t)}$$

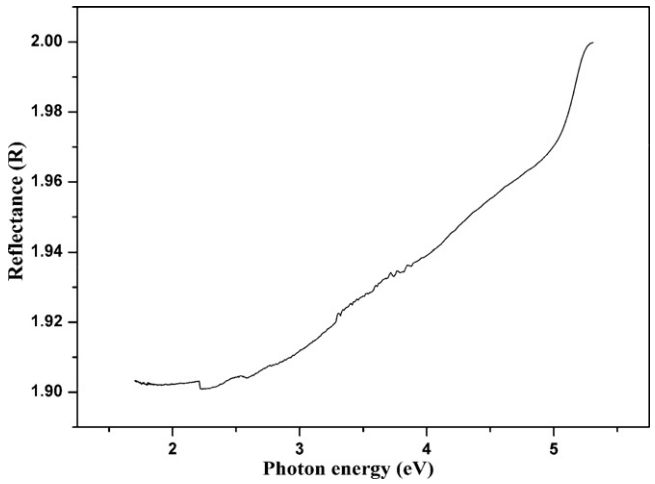

Fig. 7. Plot of reflectance (R) versus photon energy ($h\upsilon$).

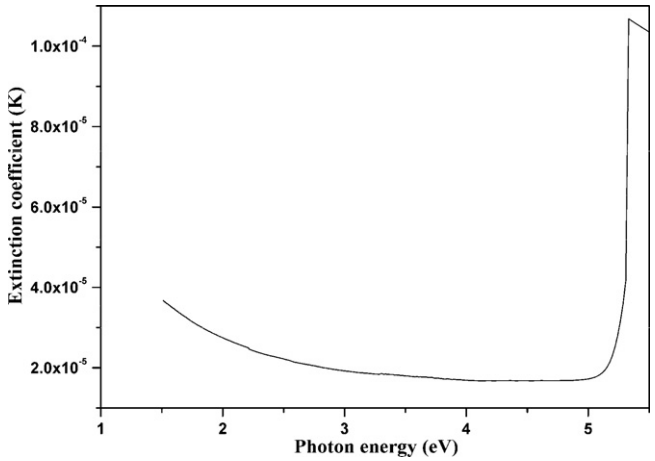

Fig. 8. Plot of extinction coefficient (K) versus photon energy ($h\upsilon$).

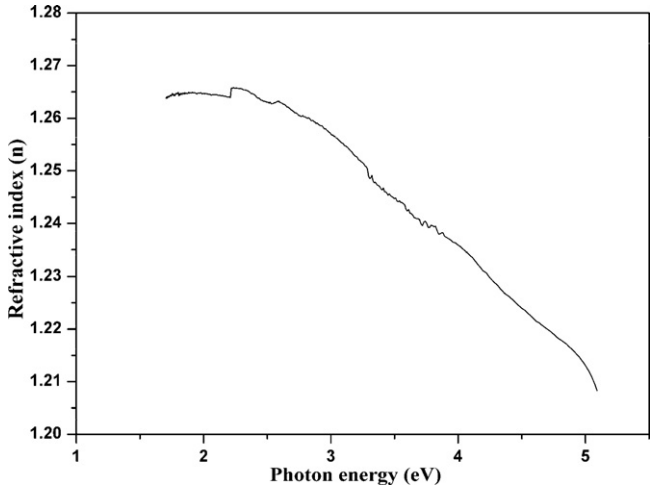

Fig. 9. Plot of refractive index (n) versus photon energy ($h\upsilon$).

From the above equation, the refractive index (n) can also be derived as

$$n = -\frac{(R+1) \pm \sqrt{3R^2 + 10R - 3}}{2(R-1)}$$

Figs. 7–9 show the variation of reflectance (R), extinction coefficient (K) and refractive index (n) as a function of photon energy ($h\upsilon$), respectively. From the above graphs, it is clear that the reflectance, extinction coefficient and refractive index depend on the photon energies. Since the internal efficiency of the device also depends on the photon energy, by tailoring the photon energy one can achieve the desired material to fabricate the optoelectronic devices.

The calculated refractive index (n) is 1.274 at 1000 nm for γ-glycine crystal.

The electric susceptibility (χ_c) can be estimated with the help of optical constants, according to the following relation [29]

$$\epsilon_r = \epsilon_0 + 4\pi\chi_c = n^2 - K^2$$

$$\chi_c = \frac{n^2 - K^2 - \epsilon_0}{4\pi}$$

where (ϵ_0) is the dielectric constant in the absence of any contribution from free carriers. The calculated value of electric susceptibility χ_c is 0.1292 at $\lambda = 1000$ nm.

The real (ϵ_r) and imaginary (ϵ_i) parts of the dielectric constant can be calculated from the following relations

$$\epsilon = (n + iK)^2$$

$$\epsilon = n^2 - K^2 + 2ink = \epsilon_r + i\epsilon_i$$

where $\epsilon_r = n^2 - K^2$ and $\epsilon_i = 2nk$

The value of real (ϵ_r) and imaginary (ϵ_i) dielectric constants at $\lambda = 1000$ nm are 1.62 and 1.05×10^{-4}, respectively. The estimated values are in good agreement with the reported values [30,31].

3.6. Thermal studies

The thermo gravimetric analysis (TGA) and differential thermal analysis (DTA) were used to study the chemical decomposition, phase transition temperature, melting point and the weight loss of the grown crystals. The grown γ-glycine in the medium of magnesium chloride was subjected to thermal analysis using SDT Q 600 thermal analyzer. For this study, a crystal in powder form weighing about 2.5370 mg was taken in a platinum crucible and analyses were carried out in an atmosphere of nitrogen at a heating rate of 20 °C min^{-1} in the temperature range 20–800 °C. The obtained TGA/DTA curves are illustrated in Fig. 10.

TGA curve shows that there is no weight loss up to 221.34 °C. Hence, the crystal is devoid of any physically adsorbed water on

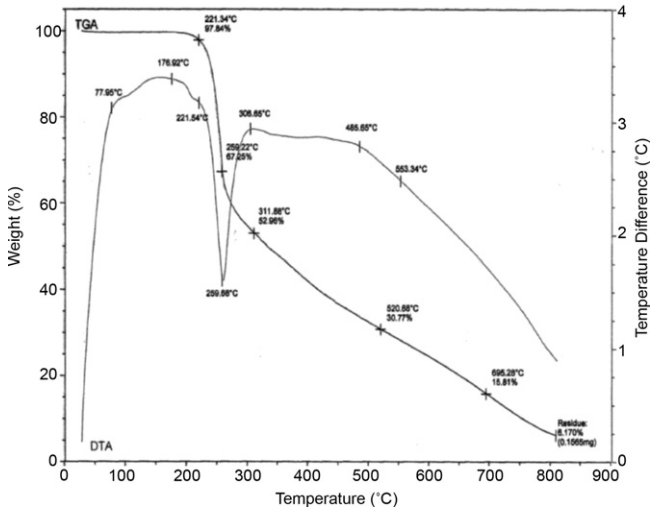

Fig. 10. TGA/DTA profile.

Table 3
Comparison of SHG efficiency of γ-glycine grown from various solvents.

Solvent	SHG efficiency with relative to KDP	Reference
Water and $NaNO_3$	1.60	[12]
Water and lithium acetate	3.40	[13]
Phosphoric acid	1.30	[14]
Water and lithium bromide	3.00	[15]
Water and strontium chloride	1.06	[21]
Water and $MgCl_2$	6.00	Present work

it. From the analysis of DTA curve, it is observed that there is a sudden weight loss occurring at temperature 259.58 °C, which indicates that rapid decomposition takes place at that temperature. γ-Glycine is thermodynamically most stable polymorphic form at ambient temperature. From TGA thermogram, it is also observed that the reduced weight percentage of about 97.64% observed at 221.34 °C may be attributed to the loss of lattice water. The major weight loss occurs between 221.34 and 259.22 °C. The resulting residue gives a weight loss for a wide range of temperatures between 259.22 °C and 695.28 °C. The weight loss corresponds to 6.170% and 0.1565 mg of residue remains [32]. Thus, from the above analyses, it is concluded that the material can be exploited for NLO application up to 213.08 °C.

3.7. SHG measurements

The classical powder method developed by Kurtz and Perry [33] was performed to estimate the NLO relative conversion efficiency of grown crystal in the fine powder form. It is a popular and powerful tool for the initial screening made to evaluate the conversion efficiency of NLO material. For this, a Q-switched Nd:YAG laser (DRC11) was used as light source. A laser beam of fundamental wavelength 1064 nm, pulse width of 10 ns with a repetition rate of 10 Hz was made to fall normally on the sample. The crystal of γ-glycine was made into a fine powder containing particles of uniform size and then packed in a micro capillary tube of uniform bore and exposed to laser radiation. The emission of green radiation (λ = 532 nm) from the crystal confirmed the second harmonic signal generated of the crystalline sample. The γ-glycine second harmonic signal of 150 mV was obtained, while the KDP gave an SHG signal of 25 mV for the same input laser energy incident on the powder sample. Thus, the SHG relative efficiency of γ-glycine crystal was found to be 6 times higher than that of KDP. The SHG efficiency of γ-glycine grown in the present study is in Table 3, which shows that it is higher than the reported values. The main contributions to the higher nonlinear optical properties of γ-glycine are the hydrogen bond and its vibrational part due to the very intense infrared bands of the hydrogen bond vibrations [34]. The high polarizing power of magnesium chloride plays an important role in the enhancement of SHG efficiency of the γ-glycine crystal grown in the present study.

4. Conclusions

Single crystals of γ-glycine in the presence of magnesium chloride aqueous solution was grown at room temperature by using slow evaporation technique. The high resolution X-ray rocking curve measurements substantiate the good quality of the grown crystal. Single crystal XRD, powder XRD and FTIR spectra analyses confirm the fact that the existence of glycine in the γ-phase. The concentration of Mg element present in the single crystal on γ-glycine can be determined by ICP-OES analysis. The UV–vis–NIR absorption spectrum reveals that the γ-glycine crystals are highly transparent in the region of 238–1200 nm. This study helped to calculate the optical constants such as absorption coefficient (α), extinction coefficient (K), refractive index (n), electric susceptibility (χ_c) and dielectric constant as a function of photon energy ($h\nu$). The thermal behavior of the grown crystal was studied by TGA/DTA. Kurtz–Perry powder SHG test confirmed the frequency doubling of the grown crystal and it efficiency was 6 times higher than that of KDP. Hence, γ-glycine grown in the presence of magnesium chloride becomes a promising material for laser application and fabrication of electro optic devices.

Acknowledgements

The authors are thankful to Prof. P. Ramasamy, SSN College of Engineering, Chennai for his fruitful discussion with us. We also thank Prof. P.K. Das, Department of Inorganic and Physical Chemistry, Indian Institute of Science, Bangalore, India. They would similarly like to express their gratitude to the Sophisticated Analytical Instrument Facility (SAIF), Indian Institute of Technology, Chennai and the Central Electrochemical Research Institute (CECRI), Karaikudi for their permission to use the facilities therein for characterizing the crystal. The authors are highly grateful to Dr. (Ms.) K.V. Rama, Technical Officer Grade-I, SAIF, IIT, Chennai for extending ICP-OES facility.

References

[1] D.R. Askeland, P.P. Phule, The Science and Engineering of Materials, Thomson, 2003.
[2] R.W. Munn, C.N. Ironside, Principle and Applications of Nonlinear Optical Materials, Chapman & Hall, London, 1993.
[3] R.A. Kumar, R. Ezhilvizhi, N. Vijayan, D.R. Babu, Physica B 406 (2011) 2594.
[4] T. Kaino, B. Cai, K. Takayama, Adv. Funct. Mater. 12 (2002) 599.
[5] H. Ringertz, Acta Crystallogr. B 27 (1971) 285.
[6] Y. Litaka, Acta Cryst. 14 (1961) 1.
[7] A. Dawson, D.R. Allan, S.A. Belmonte, S.J. Clark, W.I.F. David, P.A. McGregor, S. Parsons, C.R. Pulham, L. Sawyer, Cryst. Growth Des. 5 (2005) 1415.
[8] E. Bodyreva, Cryst. Growth Des. 7 (2007) 1662.
[9] P.G. Jonson, A. Kvick, Acta Crystallogr. B 27 (1972) 2237.
[10] L.F. Power, K.E. Turner, F.H. Moore, Acta Crystallogr. B 32 (1976) 11.
[11] Y. Litaka, Acta Crystallogr. 11 (1958) 225.
[12] M.N. Bhat, S.M. Dharmaprakash, J. Cryst. Growth 242 (2002) 245.
[13] P.V. Dhanaraj, N.P. Rajesh, Mater. Chem. Phys. 115 (2009) 413.
[14] R. Parimaladevi, C. Sekar, Spectrochim. Acta A 76 (2010) 490.
[15] T. Balakrishnan, R. Ramesh Babu, K. Ramamurthi, Spectrochim. Acta A 69 (2008) 1114.
[16] K. Lal, G. Bhagavannarayana, J. Appl. Cryst. 22 (1989) 209.
[17] G. Bhagavannarayana, S.K. Kushwaha, J. Appl. Cryst. 43 (2010) 154.
[18] G. Bhagavannarayana, P. Rajesh, P. Ramasamy, J. Appl. Cryst. 43 (2010) 1372.
[19] Oxford Diffraction, CrysAlis PRO, Oxford Diffraction Ltd, Yarnton, England, 2009.
[20] G.M. Sheldrick, Acta Cryst. A 64 (2008) 112.
[21] M. Anbuchezhiyan, S. Ponnusamy, S.P. Singh, P.K. Pal, P.K. Datta, Cryst. Res. Technol. 45 (2010) 497.
[22] A. Detcheva, N. Daskalova, S. Velichkov, I. Havezov, Spectrochim. Acta B 58 (2003) 1481.
[23] S. Sankar, M.R. Manikandan, S.D. Gopal Ram, T. Mahalingam, G. Ravi, J. Cryst. Growth 312 (2010) 2729.
[24] R. Robert, C.J. Raj, S. Krishnan, S.J. Das, Physica B 405 (2010) 20.
[25] M.A. Kaid, A. Ashour, Appl. Surf. Sci. 253 (2007) 3029.
[26] J. Gottesman, W.F.C. Ferguson, J. Opt. Soc. Am. 44 (1954) 368.
[27] A. Ashour, H.H. Afifi, S.A. Mahmoud, Thin Solid Films 248 (1994) 253.
[28] S. Suresh, A. Ramanand, P. Mani, K.M. Anand, J. Optoelectron. Biomed. Mater. 1 (2010) 129.
[29] V. Gupta, A. Mansingh, J. Appl. Phys. 80 (1996) 1063.
[30] G.A. Babu, P. Ramasamy, Curr. Appl. Phys. 10 (2010) 214.
[31] G.A. Babu, K. Thirupugalamani, P. Ramasamy, Cryst. Res. Technol. 44 (2009) 675.
[32] T.P. Srinivasan, R. Indirajith, R. Gopalakrishnan, J. Cryst. Growth 318 (2011) 762.
[33] S.K. Kurtz, T.T. Perry, J. Appl. Phys. 39 (1968) 3798.
[34] B.N. Moolya, A. Jayarama, M.R.S. Kumar, S.M. Dharmaprakash, J. Cryst. Growth 280 (2005) 581.